

# 이방향성 회전 직교축 모델을 이용한 철근콘크리트 면부재의 비선형 유한요소해석

## Nonlinear Finite Element Analysis of Reinforced Concrete Planar Members Using Rotating Orthotropic Axes Model

박 홍 근\*  
Park, Hong-Gun

### 요 약

이 연구의 목적은 단조하중과 반복하중을 받는 철근콘크리트 면부재 해석에 대한 이방향성 회전 직교축 모델의 성능을 검토하기 위함이다. 여기서 다루는 구조부재는 철근에 의하여 적절히 보강된 보, 기둥, 보-기둥 접합부, 그리고 전단벽등으로 부재의 파괴가 인장균열후 압축파괴에 의하여 일어나는 부재이다. 보통 단조하중에 대하여 사용도는 이방향성 회전 직교축 모델을 반복하중에 대하여 확장하며, 철근과 부재의 기존 재료모델과 함께 유한요소해석에 사용한다. 단조하중에 대하여 이방향성 회전 직교축 모델을 사용한 해석 결과는 취성파괴를 나타내는 철근콘크리트보의 실험결과와 비교된다. 또한 반복하중을 받는 전단벽의 극한하중, 비선형 변형, 핀칭 현상 등에 대하여 실험결과와 비교된다.

### Abstract

The objective of this research is to investigate the effectiveness of rotating orthotropic axes model in analyzing reinforced concrete planar members under cyclic as well as monotonic loading. The structural members to be addressed are moderately reinforced beams, columns, beam-column joints, and shear walls, whose failure occurs due to compressive crushing after extensive crack propagation. The rotating orthotropic axes model which is usually used for monotonic loading is developed for cyclic loading. With the existing cyclic material models of reinforcing steel and bond-slip, this material model is used for the finite element analysis. For monotonic loading, the analytical results of the rotating orthotropic axes model are compared with reinforced concrete beams which have brittle failure. For Shear wall members under cyclic loading, the analyses are compared with the experiments for the ultimate load capacity, nonlinear deformation, and pinching effect due to crack opening and closing.

\* 미국 텍사스 오스틴소재 텍사스 대학교 연구원

이 논문에 대한 토론을 1996년 6월 31일까지 본 학회에 보내주시면 1996년 12월호에 그 결과를 게재하겠습니다.

## 1. INTRODUCTION

Orthotropic axes models are frequently used for the analyses of reinforced concrete members because of the simplicity of the model. The simplicity lessens difficulty in numerical calculation due to complexity of concrete behavior. Though several researchers tried to use this approach for multiaxial compression, it is believed that the orthotropic axes model is able to produce reliable results only for tension-compression stress field.

The orthotropic axes models using equivalent uniaxial stress-strain curves are classified into fixed and rotating orthotropic axes models, based on the idealization of crack orientation. In the fixed orthotropic axes model, the cracked concrete behavior is defined by the shear stiffness and the equivalent uniaxial stress-strain curves in the orthotropic axes which is fixed to the initial direction. On the other hand, the rotating orthotropic axes model defines concrete behavior in the orthotropic axes which continuously rotate to current principal axes.

For moderately reinforced concrete members whose failure occurs due to compressive crushing after extensive cracking, the rotating orthotropic axes model produces better agreement with the experiments than the fixed orthotropic axes model. In the fixed orthotropic axes model, the compressive behavior as well as tensile behavior is defined in the fixed orthotropic axes though the principal stress axes still rotate after cracking. Therefore, the equivalent uniaxial stress-strain relation and the reduced shear stiffness in fixed orthotropic axes can not produce the crushing strength of concrete in the principal axes. However, the fixed orthotropic axes model can produce reasonable results for tensile cracking failure with-

out compressive crushing. Also, because of the fixed orthotropic axes, it is not applicable for cyclic behavior.

In the rotating orthotropic axes model, concrete cracking is not idealized by a crack direction. Instead, it is assumed that concrete cracking occurs progressively as the principal axes rotate. The progressive cracking process due to primary and secondary cracking and the surface contact between existing cracks continuously imparts behavioral directionality of concrete in rotating principal axes. Thus, the orthotropic axes rotate to the principal axes during loading. The rotating axes model does not present the directional characteristics of tensile cracks which is clearly observed in plain concrete members. However, for moderately reinforced concrete members, it can follow the rotation of the principal axes due to wide-spread progressive tensile cracking. As a result, under tension-compression, the rotating orthotropic axes model can follow the compressive behavior as well as tensile behavior in principal axes.

Because of the rotation of the orthotropic axes, this approach is applicable for cyclic behavior. However, the rotating orthotropic axes models which are usually used for monotonic loading, treat the maximum strain as the material damage regardless of the orientation of orthotropic axes. Such material models produce unrealistic behavior under reversed cyclic loading, making the damage of tensile cracks rotate by 90 degrees. In the material model developed here, the material damage surfaces of compression and tension are defined in two-dimensional stress field so that the material damage depends on the orientation of the orthotropic axes.

On the basis of smeared crack and smeared reinforcement, this research is concentrated

developing the orthotropic axes model under tension-compression of biaxial stress fields, and on predicting the complete behavior up to structural failure of reinforced concrete planar members under cyclic as well as monotonic loading. The structural members to be addressed are beams, columns, beam-column joints, and shear walls, whose behavior is affected by well-distributed cracks rather than a dominant crack, and which is not significantly affected by multiaxial compression.

The orthotropic axes model is used in finite element analysis with existing cyclic models of reinforcing steel and bond-slip. Also, a reliable and efficient solution scheme is developed for predicting complete structural behavior by investigating available nonlinear solution strategies, iteration strategies, and convergence criteria. The analysis program incorporating the material models and the solution scheme is tested to predict the behavior of structural members under monotonic and cyclic loading.

## 2. ROTATING ORTHOTROPIC AXES MODEL

The two-dimensional stress-strain relation is defined by two equivalent uniaxial stress-strain curves in orthotropic axes. Assuming that principal stress axes coincide with principal strain axes, the orthotropic axes rotate to current principal axes during loading history. The equivalent uniaxial stress-strain curve consists of envelope curves (loading curve) and unloading-reloading curves connecting the envelope curves at the compressive and tensile damage surfaces (see Fig. 1). The assumption that principal stress axes coincide with principal strain axes, used by Vecchio and Collins<sup>12)</sup>, produces reasonable results for moderately reinforced concrete which has well-distributed tensile cracks. The assumption reduces diffi-

culty in nonlinear numerical calculations, and it satisfies the behavioral requirement under cyclic loading that principal stress axes coincide with principal stress axes as the cracks close.

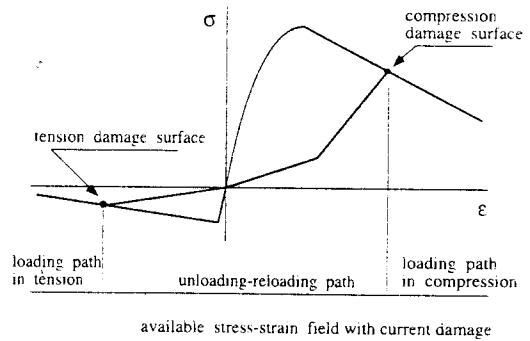


Fig. 1 Equivalent uniaxial stress-strain curve

### 2.1 Envelope Curves in Tension and Compression

In reinforced concrete, the microcracks composing the primary crack are not uniformly oriented; they deviate from the principal tensile direction. Therefore, as the cracks widen, the concrete struts are disconnected and finally crush (see Park<sup>7)</sup>). In other words, the deviation of microcracks from the principal axes reduces the effective area of the concrete struts. The compressive strength of concrete decreases due to the crack opening.

For this phenomenon, the equation of compression softening proposed by Vecchio and Collins<sup>12)</sup> is used in the compressive envelope curve. According to their proposed stress-strain relation, the compressive strength in a compressive principal axis decreases as the principal tensile strain representing the current crack width increases in the orthogonal principal tensile axis.

$$\sigma_c^u = \frac{f'_c}{0.8 - 0.34(\epsilon_t / \epsilon_t^u)} \text{ and } \sigma_c^u \leq f'_c, \quad (1)$$

where  $f'_c$  is the cylinder strength,  $\sigma_c^u$  is the compressive strength,  $\epsilon_c^u$  is the compressive strain corresponding to  $\sigma_c^u$ , and  $\epsilon_t$  is the principal tensile strain.

To idealize the two-dimensional tension stiffening stress-strain relation, it is assumed that each reinforcement layer has its own tension stiffening stress corresponding to the tensile strain in the reinforcement direction (see Fig. 2(a)). The effect of the hypothetical tension stiffening stress  $\sigma_{ts}$ , on the principal tensile stress axes is defined as follows (see Fig. 2 (b)):

$$\sigma_{tp} = \frac{1}{\rho} \sum (\rho_i \cos^2 \theta_i \sigma_{ts} \sqrt{\cos \theta_i}), \quad (2)$$

where  $\sigma_{tp}$  is the equivalent tension stiffening stress in the current principal tensile axis,  $\rho_e = \sum \rho_i \cos^2 \theta_i$ , and  $\theta_i$  is the angle between the current principal tensile axis and the reinforcement direction.

In Fig. 2(b), for tension softening without reinforcement,

$$\epsilon_{pf} = \frac{2 G_t}{h f_{cr}}, \quad (3)$$

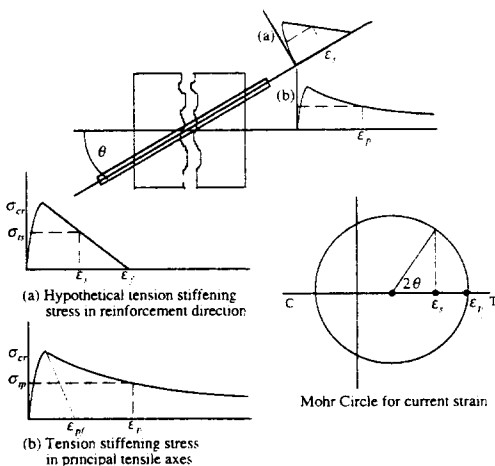


Fig. 2 Proposed tension stiffening model

where  $G_t$  is the fracture energy of tensile cracking, and  $h$  is the effective length corresponding to a Gauss point.

### 2.2 Damage Surfaces in Compression and Tension

Most rotating orthotropic axes models for cracked concrete regard the absolute value of the previous maximum strain as the only index of material damage. If the orthotropic axes rotate during loading history, using the absolute value causes the rotation of the material defects under general loading. This is controversial because a concrete crack has a certain directionality and can not rotate. Using the stress-strain relation of cracked concrete (equivalent uniaxial stress-strain state), this research simplifies the damage history of cracked concrete in tension-compression.

In the proposed cracked concrete model, under tension-compression, the uniaxial compressive stress-strain relation is maintained in a rotating principal compressive axis. Assuming that the compressive damage due to crushing is isotropic, the compression damage can be defined by the absolute value of the maximum principal compressive strain in any principal compressive axis. Accordingly, the damage surface in compression is uniform in all directions (see Fig. 3)

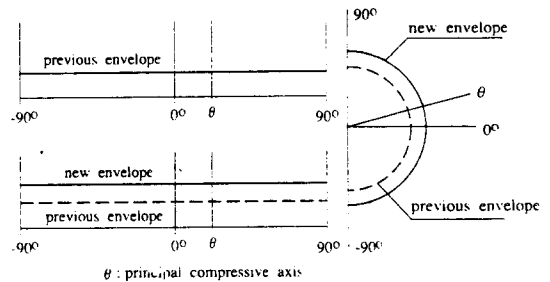


Fig. 3 Compression damage surface

On the other hand, tensile cracking damage is obviously limited to the current principal tensile axis and the neighboring directions. In the proposed model, the damage in the neighboring directions is defined by the damage influence surface due to current tension cracking or principal tensile strain. If a principal tensile strain exceeds the tension damage surface, the tensile strain forms its damage influence surface within 30 degrees in either side of the current principal tensile axis. The damage influence surface is defined by

$$\epsilon_{t\Delta\theta}^m = \epsilon_t^m \cos(3\Delta\theta), \quad (4)$$

where  $\epsilon_t^m$  is the maximum strain in the current principal tensile axis, and  $\epsilon_{t\Delta\theta}^m$  is the maximum strain in the direction  $\Delta\theta$  away from the current principal tensile axis. The tension damage surface expands to include the current damage influence surface. Since the damage influence surface is not uniform, the tension damage surface is anisotropic, unlike the compression damage surface. In eight reference directions, if the damage influence surface due to current principal tensile strain exceeds the tension damage surface, the tension damage surface expands to the current damage influence surface (see Fig. 4). The maximum strain in a principal tensile axis is linearly interpolated

between the maximum strains or the tension damage surface in the reference directions.

According to the progression of concrete damage, the cyclic behavior of cracked concrete is classified into five developmental stages in Fig. 5:

- I) Elastic range without permanent damage:
- II) Initial tension damage without compression damage:
- III) Initial compression damage without tension damage:
- IV) Damage in both tension and compression after initial tension damage; and
- V) Damage in both tension and compression after initial compression damage.

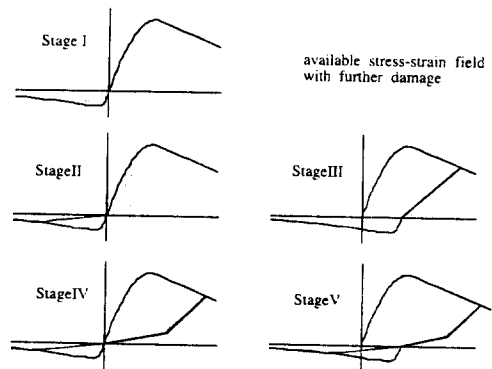


Fig. 5 Development of concrete damage

### 3. IMPLEMENTATION OF FINITE ELEMENT METHODS

In addition to the proposed cracked concrete model, existing material models of reinforcing steel and bond-slip are implemented in the finite element analysis program. To idealize reinforcing steel behavior, a strain hardening model including the bauschinger effect is used, as proposed by Brown and Jirsa.<sup>3)</sup> Reinforcing steel is idealized by either discrete or smeared elements. The bond-slip model proposed by

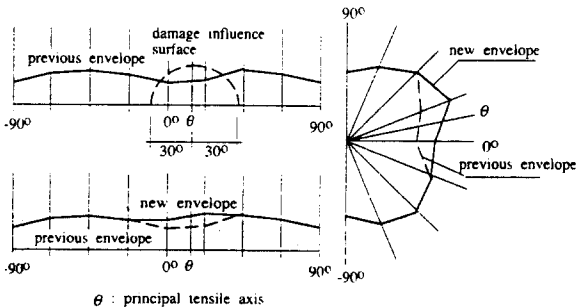


Fig. 4 Tension damage surface

Ciampi et al.<sup>4)</sup> is used; it idealizes the bond deterioration due to cyclic loading. The bond-slip elements, which are out-of-plane rectangular elements, connect the in-plane rectangular elements representing concrete and smeared reinforcement, to line elements representing discrete reinforcement.

A simplified displacement-control method (see Ramm<sup>8)</sup>) is used for the nonlinear numerical procedure, and the Newton-Raphson method with tangent stiffness is used for iteration. As a convergence tolerance limit, an incremental displacement criterion is applied.

4. APPLICATION OF PROPOSED ANALYSIS METHOD

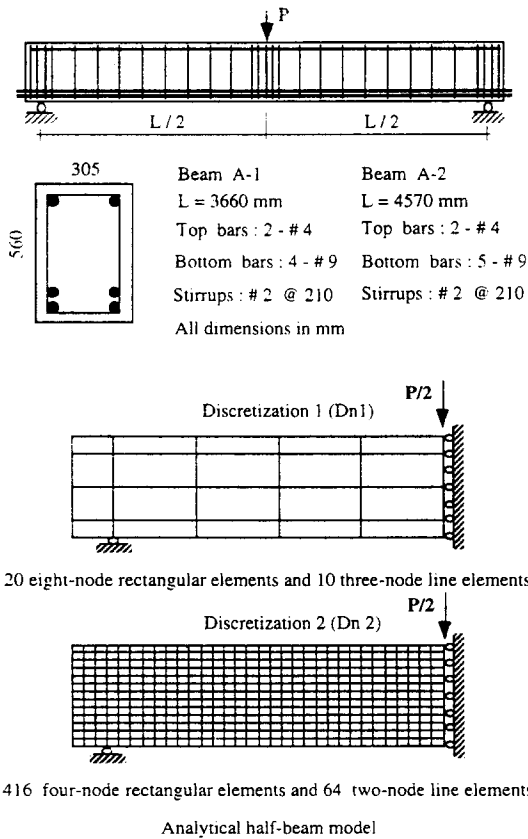


Fig. 6 Reinforced concrete beam tested by Bresler and Scordelis

4.1 Reinforced Concrete Beam Tests under Monotonic Loading (Bresler and Scordelis)

Bresler and Scordelis<sup>2)</sup> investigated the shear capacity of a series of beam specimens. The properties and the analytical model of their Beams A-1 and A-2 are shown in Fig. 6. These beams have heavy longitudinal reinforcement at the bottom, so that inelastic flexural deformation due to yielding of reinforcing steel is prevented. On the other hand, the reinforcement ratio of the vertical bars is low, inviting a shear failure due to diagonal tension cracking. Also, Discretizations 1 and 2 of the analytical half beam are shown in Fig. 6.

As shown in Fig. 7, the analytical results using the proposed approach agree well with the experiments. The load capacity of the

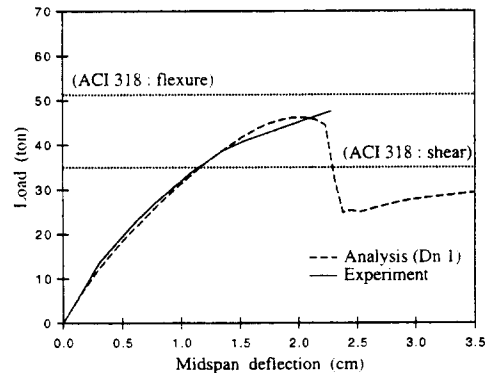
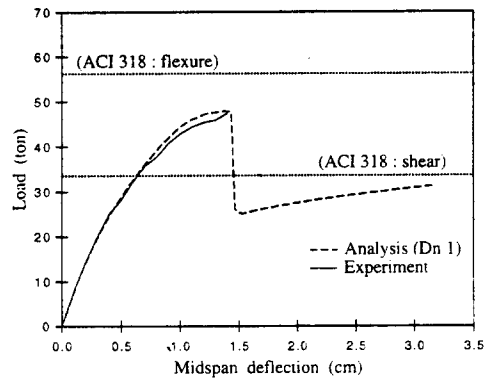


Fig. 7 Comparison between analysis and experiment of reinforced concrete beam (Bresler and Scordelis)

beam falls between the flexural and the shear load capacity values calculated according to ACI 318-89.<sup>1)</sup> The results clearly show that heavy reinforcement in flexure and lack of shear reinforcement causes shear-compression failure without much ductility. It is noted that the ACI code assumes yielding of the flexural reinforcement in tension before the complete crushing of concrete in compression.

For the tension stiffening stress in the web of the beam, the influence of the main bar in the bottom of the beam should be considered. Otherwise, the analysis underestimates the actual load capacity. This is because the diagonal crack width in the web is directly affected by the deformation of the main reinforcement in the bottom of the beam.

Fig. 8 shows the analytical results of different material models and discretizations. Both Discretizations 1 and 2 using the rotating orthotropic axes model present good agreement with the experiment. On the other hand, Discretization 2 of the fixed orthotropic axes model overestimates the ultimate strength of the beam.

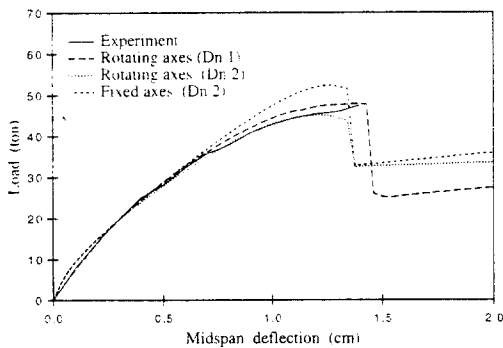


Fig. 8 Comparison between rotating and fixed orthotropic axes models

To investigate the effect of bond-slip relations on beam members, Beam A-1 is idealized as shown in Fig. 9. In the beam, all of the bot-

tom reinforcing steel bars are cut off at 30.5cm(12 inches) from the supports. In Fig. 10, the analytical results of the original beam and the modified beam are compared. The maximum load capacity of the modified beam is much lower than that of the original beam. This analysis shows that in the modified beam, the development length of the bottom steel bars is insufficient.

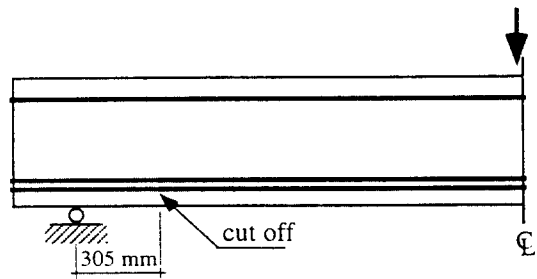


Fig. 9 Discretization of Beam A-1 for bond-slip behavior

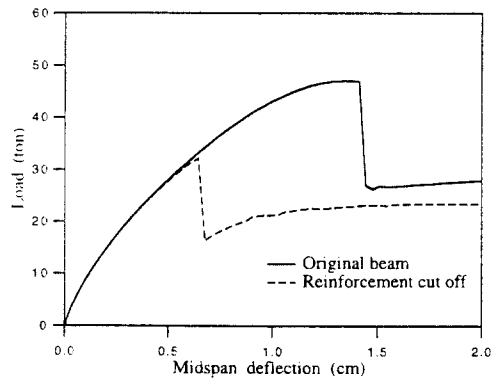


Fig. 10 Bond-slip effect on beam behavior according to development length

#### 4.2 Reinforced Concrete Masonry Wall Tests under Cyclic Loading (Shing et al.)

The proposed analytical method is applied for the reinforced concrete masonry shear wall tests performed by Shing et.al. at the University of the Colorado (see de la Rovere<sup>9)</sup>). Shing's Walls 7, 10, and 12 are analyzed here. As shown in Fig. 11, the shear walls have a rigid

base and a top slab. They are subjected to uniformly distributed vertical loads and a concentrated horizontal load at the top slab. The vertical loads remain constant during loading, while the lateral load varies. The shear walls are reinforced by uniformly distributed vertical and horizontal steel layers. The loading conditions and the properties of materials are shown in Table 1. The analytical model is shown in Fig. 11.

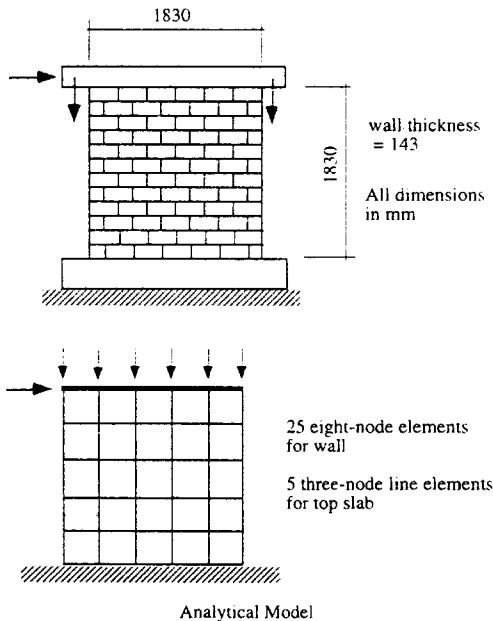


Fig. 11 Reinforced concrete masonry wall tested by Shing et al.

Table 1. Loading conditions and material properties of shear walls tested by Shing et al.

Wall No.	Masonry $\sigma'_m$ kg/cm <sup>2</sup>	Horizontal Steel		Vertical Steel		Axial load ton
		$\rho_x$ %	$f_{xy}$ kg/cm <sup>2</sup>	$\rho_y$ %	$f_{yy}$ kg/cm <sup>2</sup>	
7	205.1	0.14	3990	0/74	4925	18.2
10	225.5	0.14	3990	0.38	4433	18.2
12	225.5	0.24	4644	0.38	4433	18.2

Figures 12-14 show the cyclic load-deflection curves of Walls 7, 10, and 12. Walls 10 and 12, with similar horizontal and vertical reinforce-

ment ratios, have a maximum horizontal load capacity of 30 tons, which gradually decreases with increasing displacement. Wall 12, with more horizontal reinforcement, shows more ductile behavior than Wall 10. Wall 7, with heavy vertical reinforcement, has a large shear capacity. However, due to the relatively light horizontal reinforcement, compression crushing occurs suddenly just after the maximum horizontal load.

In Figures 12-14, analytical predictions are compared with experimental results from Walls 7, 10, and 12. For all specimens, the analytical results follow the experimental results reasonably well. This is because the well-distributed reinforcement and the vertical load prevent tensile cracks from widening; the tensile cracks spread over large area and material deterioration due to cyclic loading is minimized, which is in accordance with the assumption of the proposed material model. The analyses clearly show nonlinear deformations, the maximum load capacity, and pinching due to crack opening and closing. After the maximum member capacities reached, member behavior depends heavily on the descending slope of the compressive softening stress-strain relation of concrete. In these analyses,  $\sigma_c^f = \sigma_c^u / 20$  and  $\epsilon_c^f$

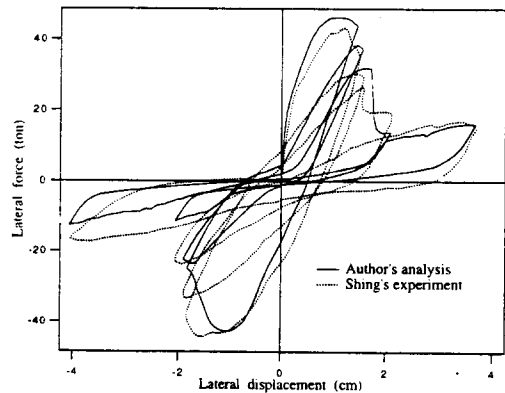


Fig. 12 Comparison between cyclic analysis experiments for Wall 7



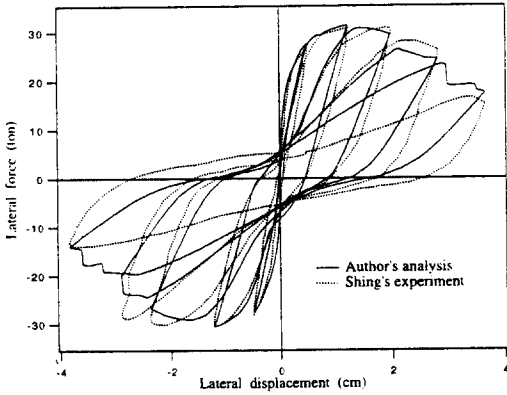


Fig. 13 Comparison between cyclic analysis and experiments for Wall 10

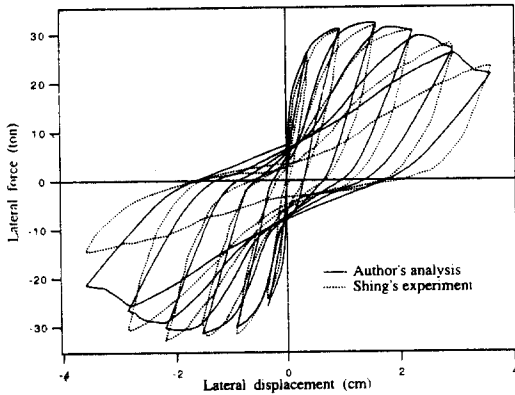


Fig. 14 Comparison between cyclic analysis and experiments for Wall 12

$=15 \epsilon_c^u$  are used, where  $\sigma_c^f$  and  $\epsilon_c^f$  are the final stress and strain.

### 5. CONCLUSIONS

The rotating orthotropic axes model reasonably defines the behavioral characteristics of reinforced concrete cracks which spread over a large area and whose width is well confined due to the influence of reinforcement. The progressive cracking process due to primary and secondary cracking and the surface contact

between existing cracks continuously imparts behavioral directionality of concrete in rotating principal axes.

The assumption that principal stress axes coincide with principal strain axes, reduces difficulty in nonlinear numerical calculation. Also, it satisfies the behavioral requirement under cyclic loading that two principal axes coincide as cracks close. The material damage surfaces of compression and tension are defined in two-dimensional stress field so that the material damage depends on the orientation of the orthotropic axes. For reversed cyclic behavior, the tensile damage surface provides multiple crack damage.

The proposed material model produces good agreement with shear-dominated behavior of reinforced concrete beams with brittle shear-compression failure. Also, the material model with the existing bond-slip model can be used to investigate the effects of anchorage length on member behavior. For shear walls under cyclic loading, the analyses show the behavioral characteristics of nonlinear deformations and the load capacity.

As far as the basic concept is concerned, the rotating orthotropic axes model proposed here can be viewed as an extension of the strut-and-tie model defined in a load-displacement field, which is frequently used as an approximate analysis and design method. However, the rotating orthotropic axes model can consider the nature of cracked concrete behavior, such as compression softening due to crack opening and tension stiffening effects. Also, since it is possible to adjust the direction of strut-and-tie to current principal axes by considering equilibrium and compatibility conditions, the proposed model reasonably produce cyclic as well as monotonic behavior.

NOTATIONS

- $\sigma_c$  = Compressive stress of concrete
- $\sigma_{cr}$  = Tensile cracking stress of concrete
- $\sigma_c^u$  = Compressive strength of concrete
- $\sigma_c^f$  = Compressive final stress of concrete
- $f_c$  = Compressive cylinder strength of concrete
- $\epsilon_c$  = Compressive strain of concrete
- $\epsilon_t$  = Tensile strain of concrete
- $\epsilon_t^m$  = Maximum tensile strain
- $\epsilon_c^u$  = Compressive strain of concrete corresponding to compressive strength  $\sigma_c^u$
- $\epsilon_c^f$  = Compressive final strain of concrete corresponding to compressive final stress  $\sigma_c^f$
- $\epsilon_c^m$  = Maximum compressive strain
- $\epsilon_p$  = Strain in current principal tensile axis
- $\epsilon_s$  = Strain in the orientation of reinforcement
- $\epsilon_t^m$  = Maximum strain in current principal tensile axis
- $\epsilon_{t\Delta\theta}^m$  = Maximum strain in the direction deviating by  $\Delta\theta$  from the current principal tensile axis
- $f_{xy}$  = Yield stress of reinforcing steel in x direction
- $f_{yy}$  = Yield stress of reinforcing steel in y direction
- $\rho_x$  = Reinforcement ratio in x direction
- $\rho_y$  = Reinforcement ratio in y direction

REFERENCES

1. ACI Committee 318, *Building Code Requirements for Reinforced Concrete(ACI-318-89)*, American Concrete Institute, Detroit, 1989.
2. Bresler, B. and Scordelis, A.C., "Shear Strength of Reinforced Concrete Beams," *American Concrete Institute Journal, Proceedings*, Vol.60,

- Jan., 1963, pp.51-72.
3. Brown, R.H. and Jirsa, J.O., "Reinforced Concrete Beams under Load Reversals," *American Concrete Institute Journal, Proceedings*, Vol. 68, May 1971, pp.380-390.
4. Ciampi, V., Eligehausen, R., Bertero, V.V. and Popov, E.P., *Analytical Model for Concrete Anchorage of Reinforcing Bars under Generalized Excitations*, Earthquake Engineering Research Center, Report No. UCB/EERC-82/83, University of California, Berkeley, 1982.
5. Darwin, D. and Pecknold, D.A., "Analysis of R/C Shear Panels under Cyclic Loading," *Journal of the Structural Division*, ASCE, Vol. 102, No. ST2, Feb., 1976, pp.355-369.
6. Karsan, I.D. and Jirsa, J.O., "Behavior of Concrete under Compressive Loadings," *Journal of the Structural Division*, ASCE, Vol.95, No.12 Dec., 1969, pp.2543-2563.
7. Park, H., *Nonlinear Finite Element Analysis of Reinforced Concrete Planar Structures*, Thesis Presented to the University of Texas at Austin, in Partial Fulfillment of the Requirements for the Degree of Doctor of Philosophy, 1994.
8. Ramm, E., "Strategies for Tracing the Nonlinear Response Near Limit Points," *Nonlinear Finite Element Analysis in Structural Mechanics*, edited by Wunderlich, W., Stein, E., and Bathe, K.J., Springer-Verlag, Berlin, 1981.
9. de la Rovere, H.L., *Nonlinear Analysis of Reinforced Concrete Masonry Walls under Simulated Seismic Loadings*, Thesis Presented to the University of California at San Diego, in Partial Fulfillment of the Requirements for the Degree of Doctor of Philosophy, 1990.
10. Stevens, N.J., Uzumeri, S.M., Collins, M.P., and Will, G.T., "Constitutive Model for Reinforced Concrete Finite Element Analysis," *American Concrete Institute Journal, Proceedings*, Vol.88, No.1, Jan., 1991, pp.49-50.
11. Stevens, N.J., Uzumeri, S.M. and Collins, P., "Reinforced Concrete Subjected to Reversed Cyclic Shear-Experiments and Constitutive Model," *American Concrete Institute Journal, Proceedings*, Vol.88, No.2, Mar., 1991, pp.

- 135-146.
12. Vecchio, F.J. and Collins, M.P., "The Modified Compression-Field Theory for Reinforced Concrete Elements Subjected to Shear," *American Concrete Institute Journal, Proceedings*, Vol. 86, No.2, Mar., 1986, pp.219-231.
13. Vecchio, F.J., *The Response of Reinforced Concrete to In-Plane Shear and Normal Stresses*, Thesis Presented to University of Toronto, in Partial Fulfillment of the Requirements for the Degree of Doctor of Philosophy, 1981.  
(접수일자 : 1995. 7. 23)